# Uptake and UV-Photooxidation of Gas-Phase Polyaromatic Hydrocarbons on the Surface of Atmospheric Water Films. 2. Effects of Dissolved Surfactants on Naphthalene Photooxidation

**Jing Chen and Kalliat T. Valsaraj***

*Cain Department of Chemical Engineering, Louisiana State University, Baton Rouge, Louisiana 70803-7303*

*Received: December 6, 2006; In Final Form: February 23, 2007*

The adsorption and photochemical transformations of gas-phase naphthalene were studied in a flow-tube reactor with a view to understanding the photochemical reactions occurring in thin water films such as those of aerosols and fogs. Suwannee River fulvic acid (SRFA) was chosen as a surrogate for the surface active humic-like substances present in atmospheric water films. Experiments were performed on both 450 and 22 $\mu$m water films over a wide concentration range of SRFA (0−1000 mg•$L^{-1}$). The effect of singlet oxygen on the reaction rate in the presence and absence of SRFA was ascertained. Naphthalene molecules can be bound to SRFA through hydrophobic interactions and be distributed in both the water and the SRFA regions. The rate constants for the photochemical reactions of naphthalene were fitted to a model that described the effect of SRFA in these two regions. The kinetic study on the 22 $\mu$m film revealed a greater surface reaction enhancement than for the 450 $\mu$m film at low SRFA concentrations. However, there was no surface reaction enhancement at high SRFA concentrations. To compare with SRFA, the effect of a conventional surfactant, sodium dodecyl sulfate, on the uptake and photochemical transformations of naphthalene was also studied.

## Introduction

Atmospheric aerosols typically contain several inorganic salts and 10−70% of organic compounds. Single particle laser mass spectrometry measurements indicate that much of the organic material in atmospheric aerosols resides at their surface.[1] The current picture of aerosols is that of a solid core coated with a thin film of water that contains surface-active organic compounds.[2,3] Thin atmospheric water films on aerosols, fogs, and ice surfaces play an important role in atmospheric chemistry, and their interfacial properties are affected to a great extent by the surface-active substances present. The types and concentrations of surface-active substances in atmospheric water films are variable.[4] They involve a variety of organic compounds such as *n*-alkanoic acids (fatty acids) and humic-like substances (HULIS).[5,6] Surface-active substances influence the state of gas−liquid interface of atmospheric aerosols by lowering their surface tension and consequently affect aerosol nucleation and growth. They also act as adsorptive surfaces for the uptake of gaseous molecules and participate in heterogeneous reactions with atmospheric radicals.[7] Extensive studies have shown that long-chain fatty acid monolayers inhibit reactive uptake of $N_2O_5$ and anthracene on water surfaces.[8−11] Understanding the effects of surface-active substances in atmospheric water films is important for elucidating the processing of organic compounds by aerosols and fogs in the atmosphere.[12]

It has been shown that thin films of water coated on surfaces are favorable reaction sites for heterogeneous transformations.[13] Of the various organic molecules present in the atmosphere, our laboratory has focused on the behavior of polycyclic aromatic hydrocarbons (PAHs) on water films and droplets. Molecular dynamics simulations have shown that gaseous PAH molecules have large free energy minima at the air−water interface, which result in substantial enrichment of PAHs at the interface.[14] Experimental work has substantiated these findings and provided evidence for the heterogeneous reactions (oxidation by ozone and photochemical oxidation) supported by the air−water interface.[10,15−20] Our most recent work concerned the UV-photochemical oxidation of naphthalene molecules adsorbed at the air−water interface.[21] We showed that the reaction products observed in the aqueous phase were mostly oxygenated products and they increased in concentration as the film thickness decreased. It was clearly established that the heterogeneous component of the reaction increased as the surface area factor increased for the water film.

Although some work has been done investigating the uptake and surface reactions of PAHs at the air−water interface, the effect of surface-active compounds in water films on the heterogeneous chemistry of PAHs remains unclear. One would expect from a review of the literature that surfactants exert several effects on the heterogeneous chemistry of gaseous species at the air−water interface. The presence of surfactants can increase the uptake rate of gaseous species; this can occur either through a micellar trapping mechanism at the surface that results in an enhanced aqueous solubility of gas species or via direct hydrogen bonding or covalent bonding between gaseous species and surface molecules. On the other hand, long-chain alcohols and acids ($C_{12}$ or larger) can decrease the permeability of gaseous species through monolayers on the aqueous surface.[22] Surfactant molecules may be involved in surface reactions with adsorbed molecules from the gas phase. Furthermore, the oxidation of the surfactant in the surface layer may present a hydrophilic surface to which uptake may not be favorable. Previous work has shown that these effects can vary with the type of surfactants forming the monomolecular films at the surface.[15]

* To whom correspondence should be addressed. E-mail: valsaraj@lsu.edu. Phone: 2255786522. Fax: 2255781476.

10.1021/jp068394p CCC: $37.00 © 2007 American Chemical Society
Published on Web 05/01/2007

**TABLE 1: Physicochemical Properties of Naphthalene, SRFA, and SDS**

| | |
|---|---|
| Naphthalene[25] | |
| mol weight | 128 g/mol |
| aq solubility at 298 K | 0.097-0.265 mmol/l |
| vapor pressure (subcooled liquid) at 298 K | 0.01-0.03 kPa |
| bulk water−air Henry's constant, $K_{WA}$, at 298 K[26,27] | 33−68 |
| octanol−water partition constant, $K_{OW}$, at 298 K | $10^{3.29}-10^{3.59}$ |
| SDS | |
| mol weight | 288.38 g/mol |
| critical micelle concn at 298 K[28] | 8 mmol/L |
| SRFA | |
| av mol weight[29] | 800 g/mol |
| elemental composn[a] | |
| carbon | 52.44% |
| hydrogen | 4.31% |
| oxygen | 42.20% |
| nitrogen | 0.72% |
| sulfur | 0.44% |
| phosphorus | <0.01% |
| soln state $^{13}$C NMR estimate of carbon distributn[30] | |
| carbonyl (220−190 ppm) | 17% |
| carboxyl (190−165 ppm) | 20% |
| aromatic (165−110 ppm) | 24% |
| Acetal (110−90 ppm) | 5% |
| Heteroaliphatic (90−60 ppm) | 11% |
| Aliphatic (60−0 ppm) | 33% |

[a] From product information provided by IHSS.

The predominant fraction of water-soluble organic compounds present in fogwaters is acidic and comprises both mono- and dicarboxylic acids and polycarboxylic acids. Polycarboxylic acids, which are the most surface-active species in fog droplets, have been found to be chemically similar to naturally occurring humic (or fulvic) acids and are referred to in the literature as HULIS. It has been shown via molecular characterization that Suwannee River fulvic acid (SRFA) is a good surrogate model to represent polycarboxylic acids in fogwaters.[5] Some studies on the effect of SRFA on PAH photodegradation in bulk water have been carried out, but the results appear conflicting. Fasnacht and Blough[23] reported that photoreactivities of PAHs in bulk water solutions were not affected by SRFA. However, other reports showed that whereas the photodegradation of benzo[*a*]pyrene and benzo[*a*]anthracene were slowed by HULIS in water, that of naphthalene increased.[24] In this work, we chose SRFA to study the effect of dissolved surfactants on PAH photooxidation in thin water films. To compare the result with conventional surfactants, we also conducted separate experiments using sodium dodecyl sulfate (SDS) as the water-soluble surfactant. As we saw in our earlier work on pure water films,[21] the air−water interface and the bulk-phase reactions occur at different rates and reactions on thin films are predominantly surface reaction limited. SRFA shows multiple effects on naphthalene photooxidation and its presence results in a different photooxidation rate compared to that in pure water films.

## Experimental Section

**Materials.** Naphthalene (≥99%) was obtained from Aldrich. SRFA was obtained from the International Humic Substances Society (Cat. No. 1S101F). SDS (≥99.5%) was obtained from Gibco BRL (Grand Island, NY). All chemicals were used as received. Table 1 lists the physicochemical properties of naphthalene, SRFA, and SDS.

**Uptake and Photooxidation of Naphthalene.** The system used for the uptake and photooxidation of naphthalene on SRFA films was identical with that described previously.[21] Briefly, a naphthalene vapor/air mixture was introduced to a horizontal flow-tube reactor at a total flow rate of 100 $cm^3 \cdot min^{-1}$ and naphthalene adsorbed onto a SRFA aqueous film coated on a $3.5 \times 92$ cm glass trough inside of the flow-tube reactor. After the aqueous concentration of naphthalene ceased increasing indicating that partition equilibrium was achieved between the gas and liquid phases, two UV lamps on top of the flow-tube reactor were switched on, delivering UV light with wavelengths that ranged between 280 and 315 nm and peaked at 302 nm. The UV light intensity on the surface of the SRFA solution film was 1.85 $W \cdot m^{-2}$. Photoreaction of naphthalene was allowed to occur for a given duration of time before samples were taken for analysis. Naphthalene vapor was continuously introduced into the reactor to compensate for loss of naphthalene during the reaction, and thus, naphthalene concentration in the liquid phase remained constant. For all uptake and photooxidation experiments, the gas-phase concentration of naphthalene was assumed constant and the reactor temperature was maintained at 296 K by a cooling bath. SRFA solutions with varying concentrations (0−949 $mg \cdot L^{-1}$) were used to make the film. The ratio of the volume to the surface area of the film was determined to be the film thickness. The film thickness was fixed at 450 $\mu$m for the uptake study while both 22 and 450 $\mu$m SRFA aqueous films were employed for photoreaction. Separate experiments using SDS as the water-soluble surfactant were also conducted. Concentrations of the SDS solutions used to make the SDS film ranged between 0 and 4100 $mg \cdot L^{-1}$.

Quantification of naphthalene and photoreaction products in the aqueous samples was done using a high performance liquid chromatography (HPLC). Identification of compounds was achieved by matching retention times of standard solutions within ±0.1 min and by matching the UV spectrum of the standards and the sample. The HPLC instrument consisted of an Agilent Technologies HPLC 1100 series with online degasser (G1322A), quaternary pump (G1311A), autosampler (G1313A), column thermostat (G1316A), and diode array detector (G1315A). An EnviroSep-PP column of 125 mm × 3.20 mm with 5 $\mu$m particle size (Phenomenex Corp., Torrance, CA) was used. The injection volume was 25 $\mu$L, and the column thermostat was set to 40 °C. The mobile phase started at 100% water (HPLC grade, EMD Chemicals Inc., Gibbstown, NJ) and held for 3 min, then ramped to 80% acetonitrile (HPLC grade, EMD Chemicals Inc., Gibbstown, NJ) and 20% water within 6 min and held at this concentration for 5 min, and finally returned to 100% water in 2 min and held for 1 min at a constant flow rate of 0.5 mL/min. The detection wavelength was set to 250 nm with 100 nm bandwidth and 4 nm slit.

**Surface Tension of SRFA Solutions.** To obtain the surface excess of SRFA, surface tensions of SRFA solutions were measured by the Wilhelmy plate method using a Krüss model K-14 process tensiometer . Surface tensions were measured at room temperature (23 °C) over a wide range of SRFA concentration (0−20 $g \cdot L^{-1}$). Deionized water was used in the preparation of all SRFA solutions.

**Light Absorption by SRFA.** SRFA solutions exhibit a significant absorption of UV−visible light, especially at high concentrations. To be able to compare the photochemical reaction rates of naphthalene in SRFA solutions to that in pure water, absorbance of SRFA solutions was measured on a Spectronic Genesys 5 UV/vis spectrophotometer at 302 nm, which is the peak wavelength of the UV light employed in the photooxidation experiments.

**Fluorescence Measurements.** The binding affinity of naphthalene to SRFA was investigated by fluorescence quenching. Fluorescence measurements were conducted on an OLIS DM

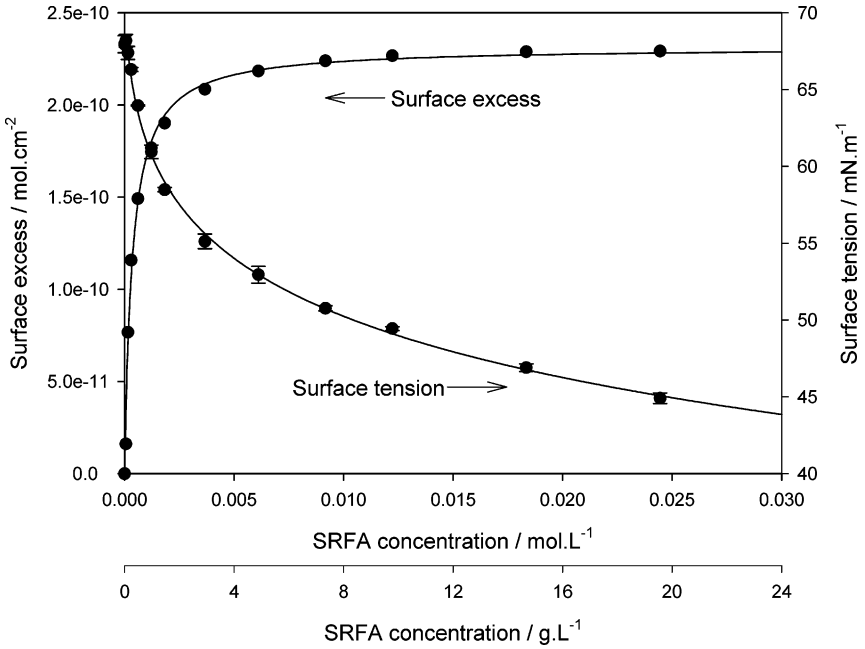


**Figure 1.** Surface tension change of the aqueous solution of SRFA. Also shown is the surface excess of SRFA at the air−water interface fitted to a Langmuir isotherm.

45 spectrofluorometer. Aqueous naphthalene solution was prepared by adding excessive solid naphthalene to deionized water and shaking the solution in a Blue M shaking bath overnight for equilibration. The solution was filtered and stored in the dark for future use. Naphthalene concentration of the stock solution was determined to be 23 mg·L$^{-1}$ by HPLC. For fluorescence measurements, 1 mL of the stock solution and 0.1 mL of SRFA solution with varying SRFA concentration were added and thoroughly mixed in a 1.25 × 1.25 × 4.5 cm PMMA cuvette and fluorescence of the mixed solution was measured at room temperature after 15 min. To serve as the background, fluorescence of solutions containing SRFA only was also measured with the same SRFA concentrations and instrumental conditions. The excitation wavelength of the fluorescence measurements was set at 286.5 nm where the maximum naphthalene fluorescence intensity was obtained. The emission wavelength ranged between 290 and 460 nm at 1-nm increments, and the peak emission wavelength was detected to be 332 nm for naphthalene and 432 nm for SRFA.

To correct for inner filter effects, absorbance measurements were taken at 286.5 and 332 nm for the same solutions used in the fluorescence measurements. The fluorescence of naphthalene was corrected for both the background fluorescence and the inner filter effect.

## Results and Discussion

**Surface Excess of SRFA.** Figure 1 shows the adsorption of SRFA on the water surface and the decrease in the air−water interfacial tension. The surface tension of SRFA solution decreased monotonically with increase in the aqueous concentration of SRFA indicating that the fulvic acid is surface active. The surface tension decreased sharply at low aqueous concentrations whereas the rate of decrease was slower at high concentrations. Previous report[31] on the surface tension of a sediment-derived fulvic acid showed that the surface tension decrease showed a distinct break at what was termed an aggregation concentration of 12.3 g·L$^{-1}$ (1.5 × 10$^{-2}$ mol·L$^{-1}$). However, no such distinct aggregation concentration was observed in the present case. From the surface tension change, the surface excess of SRFA was obtained using the Gibbs adsorption equation

$$\Gamma_S = -\left(\frac{a_S}{RT}\right)\frac{d\sigma}{da_S} \quad (1)$$

where $\Gamma_S$ is the surface excess of SRFA (mol·cm$^{-2}$), $\sigma$ is the aqueous surface tension (mN·m$^{-1}$), and $a_s$ is the activity of SRFA in the bulk solution (mol·L$^{-1}$). For dilute solutions activity is the same as concentration, $C_S$, of SRFA in the aqueous phase (mol·L$^{-1}$). The surface excess data was fitted to a Langmuir equation of the form

$$\Gamma_S = \frac{\Gamma_{max} C_S}{C_{1/2} + C_S} \quad (2)$$

As shown in Figure 1, we obtained values of $\Gamma_{max} = 2.3 \times 10^{-10}$ mol·cm$^{-2}$ and $C_{1/2} = 3.5 \times 10^{-4}$ mol·L$^{-1}$ by fitting the surface excess data to the above equation. The maximum monolayer adsorption capacity, $\Gamma_{max}$, was used to obtain the surface area occupied by an SRFA molecule, which was 0.72 nm$^2$. Reported literature values[31] are in the range 0.3−0.72 nm$^2$.

**Uptake of Naphthalene into Surfactant Films.** The uptake of naphthalene from the gas phase by a 450 $\mu$m aqueous film as a function of the aqueous phase surfactant (SRFA and SDS) concentration is shown in Figure 2. In all these cases, a constant gas-phase naphthalene concentration was maintained in the flow reactor. The uptake of naphthalene into the film is gas-phase diffusion controlled at very low gas flow rates. Previous work from our laboratory had determined that for uptake into pure water a gas flow rate >100 cm$^3$·min$^{-1}$ in the reactor was enough to eliminate the gas-phase diffusion resistance to mass transfer of naphthalene.[21] The aqueous naphthalene concentration was determined after equilibrium between the aqueous and gas phases in the flow reactor had been achieved. For most conventional surfactants such as SDS the expected trend is a minimal increase in naphthalene uptake (solubility) until the critical micelle concentration (cmc) of the surfactant is reached. Above the cmc, the micellar pseudophase in the aqueous

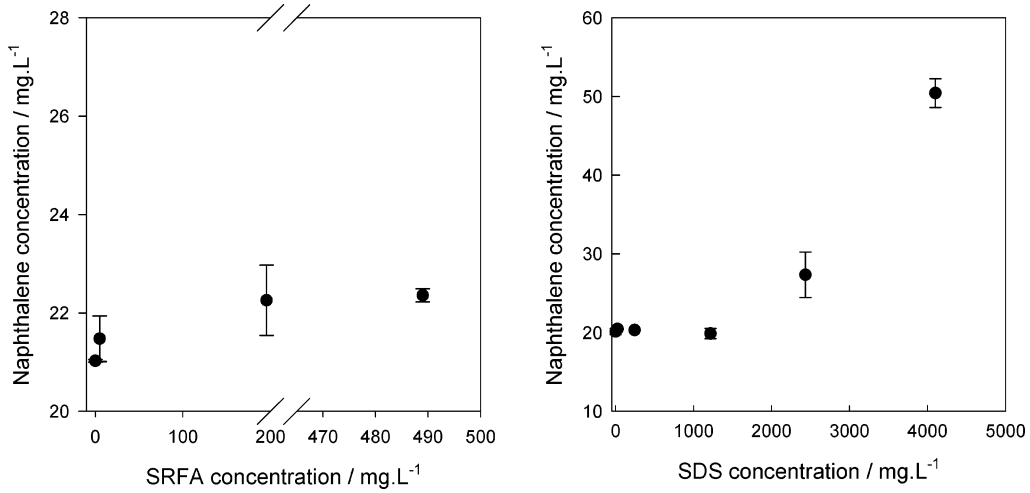


**Figure 2.** Uptake of naphthalene from the gas phase on an aqueous film (450 $\mu$m) with different surfactant (SRFA and SDS) concentrations.

**TABLE 2: Kinetic Rate Constants for Product Formation in SRFA Solution Films and Pure Water Films ($T$ = 296 K)**

| | pure water | | | | | | SRFA (18.8 mg·L$^{-1}$) | | | | | |
|---|---|---|---|---|---|---|---|---|---|---|---|---|
| | 450 $\mu$m | | | 22 $\mu$m | | | 450 $\mu$m | | | 22 $\mu$m | | |
| *compd* | $K_1$/min$^{-1}$ | $k_2$/min$^{-1}$ | $R^2$ | $k_1$/min$^{-1}$ | $k_2$/min$^{-1}$ | $R^2$ | $k_1$/min$^{-1}$ | $k_2$/min$^{-1}$ | $R^2$ | $k_1$/min$^{-1}$ | $k_2$/min$^{-1}$ | $R^2$ *a* |
| coumarin | $3.3 \times 10^{-4}$ | $3.6 \times 10^{-3}$ | 0.945 | $4.8 \times 10^{-4}$ | $2.7 \times 10^{-3}$ | 0.969 | $4.4 \times 10^{-5}$ | $6.6 \times 10^{-5}$ | 0.976 | $1.9 \times 10^{-4}$ | $1.1 \times 10^{-3}$ | 0.945 |
| phthalide | $1.1 \times 10^{-4}$ | | 0.976 | $2.8 \times 10^{-4}$ | | 0.981 | $6.2 \times 10^{-5}$ | | 0.930 | $2.0 \times 10^{-4}$ | | 0.960 |
| 1,3-indandione | $8.7 \times 10^{-5}$ | $2.2 \times 10^{-3}$ | 0.950 | $1.1 \times 10^{-4}$ | $2.2 \times 10^{-3}$ | 0.956 | $3.0 \times 10^{-5}$ | $1.6 \times 10^{-4}$ | 0.988 | $7.3 \times 10^{-5}$ | $9.3 \times 10^{-4}$ | 0.961 |
| 1-naphthol | $4.3 \times 10^{-5}$ | $3.1 \times 10^{-3}$ | 0.952 | $7.4 \times 10^{-5}$ | $5.2 \times 10^{-3}$ | 0.927 | $1.5 \times 10^{-5}$ | $1.3 \times 10^{-3}$ | 0.948 | $3.2 \times 10^{-5}$ | $1.8 \times 10^{-3}$ | 0.952 |

[a] $R^2$ is the correlation coefficient for the data fit to eq 3.

solution greatly increases the uptake and a sharp linear increase in solubility is to be expected.[32] Indeed such behavior was noted for naphthalene uptake in the presence of SDS. However, we observed that the aqueous naphthalene concentration only slightly increased at small SRFA concentrations. Only at high SRFA concentrations did the naphthalene solubility in the aqueous phase exceed the pure water solubility. No sharp increase in naphthalene uptake was noted in the case of SRFA. This is due to the lack of a critical aggregation concentration for SRFA at which a micellelike structure is formed in the aqueous phase. The observed small increase in naphthalene uptake results from the "partition-like" hydrophobic interaction between naphthalene and SRFA.

**Photochemical Reactions of Naphthalene in SRFA Aqueous Films.** Photochemical reaction kinetics of naphthalene was investigated in 450 and 22 $\mu$m water films containing SRFA. HPLC chromatograms of the reaction samples showed peaks similar to those of the pure water reaction samples. No extra peaks were observed except for the signals due to SRFA. As for the reaction in pure water, 1,3-indandione, phthalide, coumarin, and 1-naphthol were identified to be the four major photooxidation products of naphthalene in SRFA solutions. Quantification of these compounds was done on HPLC, and the reaction rate constants were obtained by fitting the kinetic data to the equation

$$C_{P1}(t) = \frac{k_1}{k_2} C_{N0}(1 - e^{-k_2 t}) \qquad (3)$$

where $k_1$ is the product formation rate constant, $k_2$ is the product reaction rate constant, $C_{P1}$ is the concentration of the product, and $C_{N0}$ is the concentration of naphthalene. The reaction scheme was $N \xrightarrow{k_1} P1 \xrightarrow{k_2} P2$. A detailed deduction of eq 3 was given in our previous work.[21] SRFA is known to strongly absorb UV−visible light. To compare the reaction rates in SRFA films and pure water films, the measured kinetic rate constants were divided by the light screening factor, $S_\lambda$, to correct for internal light filtering by SRFA.[33] $S_\lambda$ is given by

$$S_\lambda = (1 - 10^{-\epsilon_\lambda l C_S})/2.303\epsilon_\lambda l C_S \qquad (4)$$

where $\epsilon_\lambda$ is the unit absorptivity of SRFA, determined to be $1.19 \times 10^{-2}$ L·mg$^{-1}$·cm$^{-1}$ at 302 nm by the absorbance measurements, $l$ is the light path length (cm), and $C_S$ is the concentration of SRFA (mg·L$^{-1}$). The light path length was taken to be the film thickness, which yields the lower limit of the light screening factor. For the 22 $\mu$m film, the light screening factor was close to 1 in the concentration range that we investigated and light filtering by SRFA was negligible due to the small path length. However, light attenuation by SRFA in the 450 $\mu$m film was notable. To get a light screening factor of 0.95, we need a SRFA concentration of 1700 mg·L$^{-1}$ for a 22 $\mu$m film but only 85 mg·L$^{-1}$ for a 450 $\mu$m film. Therefore, light attenuation by SRFA should be taken into account for the 450 $\mu$m film. The rate constants for the 450 $\mu$m SRFA aqueous film in this work were corrected on the basis of the light screening factor.

Table 2 compares the reaction rate constants for the four products in a typical SRFA aqueous film and pure water film. As shown in Table 2, the product formation rate constants in SRFA aqueous films at $C_S$ = 18.8 mg·L$^{-1}$ were smaller than those in pure water films of the same film thickness, indicating an inhibiting effect of SRFA on naphthalene photochemical reactions at $C_S$ = 18.8 mg·L$^{-1}$. To ascertain the inhibiting effect of SRFA on naphthalene photooxidation, we conducted a series of photoreaction experiments over a wide range of SRFA concentrations (0−949 mg·L$^{-1}$). The observed formation rate constant, $k_{1,obs}$, for phthalide and coumarin in a 450 $\mu$m film as a function of the aqueous phase SRFA concentration is shown in Figure 3. Interestingly, it turns out that SRFA has multiple

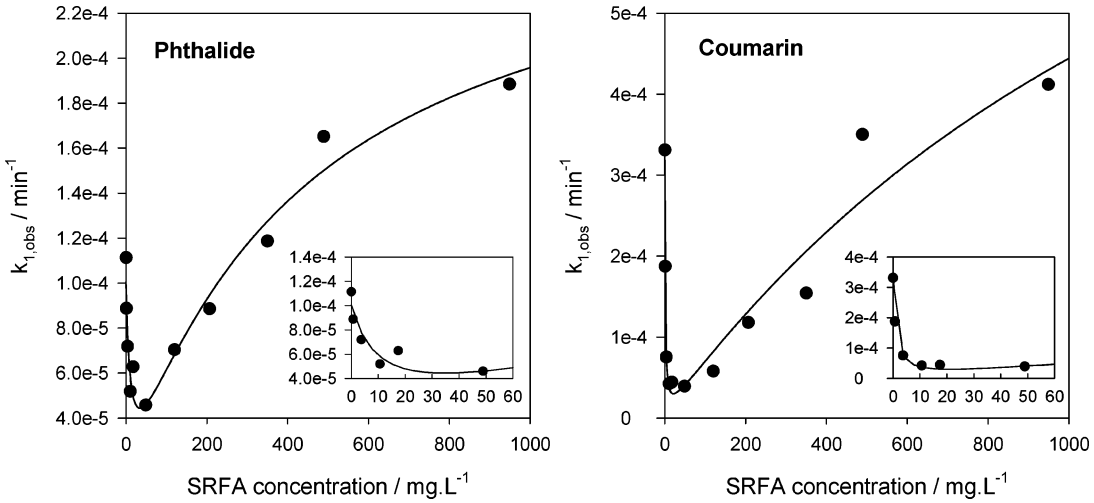


**Figure 3.** Effect of SRFA on the observed formation rate constants for phthalide and coumarin in a 450 $\mu$m aqueous film. The solid lines represent the theoretical fit to experimental data (eq 8). The insets are blowups of the data at small SRFA concentrations.

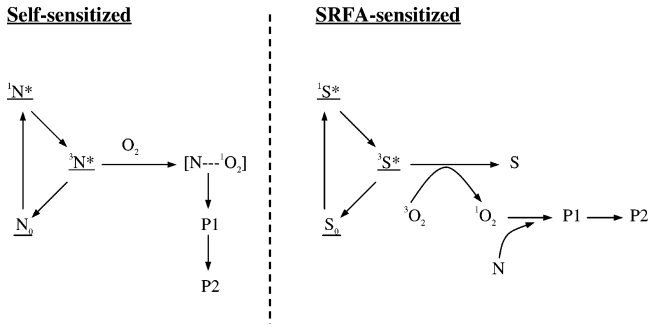


**Figure 4.** Mechanistic interpretation of naphthalene oxidation by singlet oxygen via (a) self-sensitized and (b) SRFA-sensitized pathways.

effects on naphthalene photochemical reactions instead of a single inhibiting effect. For both products, $k_{1,obs}$ initially decreased with an increase in SRFA concentration until $C_S$ reached around 50 mg·L$^{-1}$. After that, $k_{1,obs}$ began to increase with further addition of SRFA to reach an asymptotic bound.

It has been proposed in the literature that singlet oxygen ($^1O_2$) is the dominant reaction intermediate in the direct photooxidation of PAHs induced by UV light.[34,35] The PAH photooxidation mechanism by the singlet oxygen route is briefly described as follows. Under UV light, PAH molecules are excited to their singlet state, which has a very short lifetime usually on the order of 10 ns or less[33] and can decay in part to the triplet state through intersystem crossing. Energy transfer from triplet PAH molecules to dioxygen molecules produces highly reactive singlet oxygen, which reacts with ground state PAH molecules to produce oxidation products. On the other hand, UV-light absorption of humic or fulvic acid molecules can also promote them to their singlet excited-state and generate singlet oxygen via the same route as PAHs.[33,36,37] Therefore, singlet oxygen involved in the photooxidation of naphthalene in SRFA aqueous solutions can be induced either by naphthalene or by SRFA. Figure 4 shows the mechanistic scheme that depicts both self-sensitized and SRFA-sensitized photooxidation of naphthalene in SRFA aqueous solutions. In light of this mechanism, the observed photooxidation rates of naphthalene in SRFA solutions are considered to be a combined result of the self-sensitized process and the SRFA-sensitized process. The kinetic data are analyzed as follows on the basis of this hypothesis.

*SRFA-Sensitized*. PAHs are highly hydrophobic and are known to undergo complex formation with humic materials through hydrophobic interactions.[38] As a result of the association between naphthalene and SRFA, naphthalene in SRFA aqueous solutions exists in two regions: the SRFA region; the bulk aqueous region. Therefore, the product formation rate of naphthalene photooxidation sensitized by SRFA can be expressed by

$$\left(\frac{d[P]}{dt}\right)_{SRFA} = \frac{V_1}{V_{tot}} k_{rxn}[Naph]_1[^1O_2]_{1,SRFA} + \frac{V_2}{V_{tot}} k_{rxn}[Naph]_2[^1O_2]_{2,SRFA} \quad (5)$$

where $k_{rxn}$ is the bimolecular reaction rate constant of naphthalene with $^1O_2$ and $V_1$, $V_2$, and $V_{tot}$ are the volumes of the SRFA region, the bulk aqueous region, and the whole solution, respectively. The subscript SRFA denotes the contribution from the SRFA-sensitized process, and 1 and 2 denote the SRFA and the bulk aqueous phase respectively. The above equation can be coupled with the distribution of naphthalene and SRFA-induced singlet oxygen between the SRFA and the bulk aqueous region to obtain the following equation for product formation (see Supporting Information for full derivation):

$$\left(\frac{d[P]}{dt}\right)_{SRFA} = (k_{rxn}K_{OM}[^1O_2]_{1,SRFA} + k_{rxn}k_{gen})\frac{[SRFA]}{1 + K_{OM}[SRFA]}[Naph] \quad (6)$$

In this equation, $K_{OM}$ is the partition coefficient of naphthalene to SRFA and $k_{gen}$ is a kinetic constant describing the concentration of singlet oxygen in the bulk aqueous phase induced by SRFA. The term in the parentheses is a constant.

*Self-Sensitized.* Although humic substances can induce highly reactive photooxidants under UV−visible light,[39] they can also quench or scavenge the PAH excited states, free radicals, or other excited species that may be intermediates in the photochemical reactions of PAHs. Considering the self-sensitized photooxidation of naphthalene in the presence of SRFA, the predominant triplet energy of SRFA is estimated to be 250 kJ·mol$^{-1}$ [33] and is lower than the triplet energy of naphthalene (255 kJ·mol$^{-1}$ [40]). Therefore, triplet−triplet (T−T) energy transfer occurs between triplet naphthalene and ground-state SRFA to give ground-state naphthalene and triplet SRFA. In this way triplet naphthalene is quenched. T−T energy transfer is a spin-allowed process, and the quenching normally proceeds

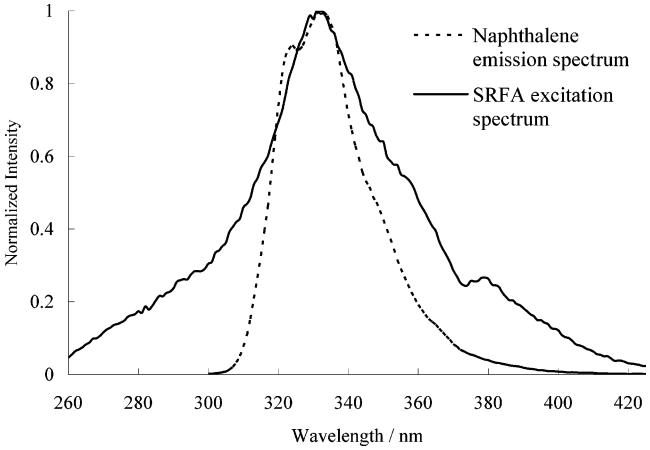


**Figure 5.** Fluorescence excitation spectrum of SRFA (4.4 mg·L$^{-1}$; detection emission wavelength, 432 nm) and fluorescence emission spectrum of naphthalene (6.5 mg·L$^{-1}$; excited at 286.5 nm).

at a diffusion-controlled rate.[40] On the other hand, Figure 5 shows the fluorescence emission spectrum of naphthalene and the fluorescence excitation spectrum of SRFA in water samples from the fluorescence measurements. Interestingly, we found that both the emission spectrum of naphthalene and the excitation spectrum of SRFA peak at 332 nm. This peak overlap suggests that singlet naphthalene molecules could also transfer their energy to ground-state SRFA molecules by fluorescence resonance energy transfer (FRET). Therefore, SRFA can not only quench triplet naphthalene via the T−T energy transfer process but also compete for the energy transferred from singlet naphthalene and inhibit the production of triplet naphthalene. As a result, the production of singlet oxygen induced by triplet naphthalene is inhibited, which consequently slows the self-sensitized photooxidation of naphthalene. Using the Stern−Volmer approach to describe the inhibiting effect of SRFA on the self-sensitized photooxidation of naphthalene, we obtain (see Supporting Information for derivation)

$$\left(\frac{d[P]}{dt}\right)_{Naph} = k_{rxn}[^1O_2]_0 \frac{1}{(1 + K_{OM}[SRFA])(1 + k_q[SRFA])}[Naph] \quad (7)$$

where $k_q$ is the quenching constant of SRFA and $[^1O_2]_0$ is the concentration of singlet oxygen in the solution without SRFA.

Combining eqs 6 and 7, we obtain the following expression that describes the dependence of the observed overall product formation rate constant on the concentration of SRFA:

$$k_{1,obs} = (k_{rxn}K_{OM}[^1O_2]_{SRFA} + k_{rxn}k_{gen})\frac{[SRFA]}{1 + K_{OM}[SRFA]} + k_{rxn}[^1O_2]_0 \frac{1}{(1 + K_{OM}[SRFA])(1 + k_q[SRFA])} \quad (8)$$

The formation rate constants of phthalide and coumarin in the 450 $\mu$m SRFA aqueous films are fitted to eq 8, and the resulting fit parameters are listed in Table 3. The correlation coefficients are 0.963 and 0.950, respectively, indicating that the fit is satisfactory. Although the correlation cannot give all the individual constants in eq 8, values of $K_{OM}$ (=$C_2$) and $k_q$ (=$C_4$) are obtained. To compare with the value of $K_{OM}$ obtained from the data correlation, we also tried to measure the partition coefficient of naphthalene to SRFA by fluorescence quenching. Unfortunately, no detectable fluorescence quenching was observed from the fluorescence measurements after the inner filter effect of SRFA was corrected. Using the average $K_{OM}$ value we obtained from the correlation, the Stern−Volmer plot for naphthalene quenching by SRFA would have a slope of 1.45 $\times$ 10$^{-3}$ L·mg$^{-1}$, which indeed is too small to be observed from the fluorescence quenching measurements.

To represent the typical water film in a fog droplet, we performed experiments on the 22 $\mu$m water film with submonolayer coverage of SRFA. According to eq 2, the surface coverage of SRFA at the highest concentration we used was 77% of full monolayer coverage. Figure 6 shows the observed formation rate constants for phthalide and coumarin on the 22 $\mu$m film. It should be noted that the photooxidation mechanism and kinetics discussed above pertained to the bulk-phase photochemical reactions of naphthalene and no surface effects were considered. For the 450 $\mu$m film that has been shown in our previous work to exhibit mainly bulk phase behavior,[21] the kinetic data was well interpreted by eq 8. However, the photochemical reactions of naphthalene on the 22 $\mu$m film were predominantly surface reaction limited[21] and it would be inappropriate to fit the kinetic data on the 22 $\mu$m film to eq 8. Thus, the data shown in Figure 6 was not fitted to eq 8. Similar to the photooxidation on the 450 $\mu$m film, the observed formation rate constants on the 22 $\mu$m film also show an initial decrease followed by an increase as the concentration of SRFA increases, consistent with the two-pathway mechanism. Moreover, SRFA exhibits a distinct effect on the surface photochemical reactions of naphthalene. Take the formation of phthalide for example. The ratio of the formation rate constant for phthalide on the 22 $\mu$m film to the corresponding rate constant on the 450 $\mu$m film increases from 2.5 in pure water to 3.3 at $C_S$ = 49 mg·L$^{-1}$ and then decreases to 1.2 at $C_S$ = 980 mg·L$^{-1}$, indicating a greater surface reaction enhancement at low SRFA concentrations than in pure water and a slight or zero surface reaction enhancement at high SRFA concentrations. Heterogeneous reactions at the gas−aqueous interface have been shown to proceed faster than homogeneous reactions in the bulk water phase, partly attributed to the enhanced surface concentrations.[21,41,42] The reasons for the greater surface reaction enhancement in the region of small SRFA concentrations are probably 2-fold. First, the presence of SRFA increases the surface concentration of naphthalene, which directly enhances the surface reaction rate. Second, as shown earlier, the self-sensitized photooxidation of naphthalene is the dominant reaction pathway at small SRFA concentrations. The presence of SRFA probably decreases the mobility of molecules on the surface and consequently suppresses the diffusion-controlled T−T energy transfer from triplet naphthalene to ground-state SRFA. Thereby the quenching effect of SRFA on the self-sensitized process is weakened and the surface reaction rate is enhanced. Unlike under low SRFA concentrations, naphthalene molecules are primarily distributed in the SRFA region at high SRFA concentrations. Humic substances have been pictured to have an open structure with a number of hydrophobic cavities where hydrophobic interactions between humic substances and hydrophobic organic compounds occur.[38] In light of this molecular level binding picture, it is speculated that naphthalene molecules bound to SRFA are "caged" in the SRFA region, regardless of whether they are on the surface or in the bulk phase. As a result, the property of the SRFA microregion determines the photochemical reactivity of naphthalene at high SRFA concentrations and no difference exists between the surface and the bulk-phase reactions.

**Photochemical Reactions of Naphthalene in SDS Aqueous Films.** To compare the effect of SRFA with conventional surfactants, photochemical reaction kinetics of naphthalene in

**TABLE 3: Parameters Obtained by Fitting the Formation Rate Constant Data to Eq 14**[a]

| source | $C_1$/L·mg$^{-1}$·min$^{-1}$ | $C_2$ (=$K_{OM}$)/L·mg$^{-1}$ | $C_3$/min$^{-1}$ | $C_4$ (=$k_q$)/L·mg$^{-1}$ | $R^2$[b] |
|---|---|---|---|---|---|
| phthalide | $6.5 \times 10^{-7}$ | $2.3 \times 10^{-3}$ | $1.0 \times 10^{-4}$ | $8.6 \times 10^{-2}$ | 0.963 |
| coumarin | $7.1 \times 10^{-7}$ | $6.0 \times 10^{-4}$ | $3.3 \times 10^{-4}$ | $9.5 \times 10^{-1}$ | 0.950 |

[a] Simplified fit equation: $k_{obs} = C_1[\text{SRFA}]/(1 + C_2[\text{SRFA}]) + C_3/(1 + C_2[\text{SRFA}])/(1 + C_4[\text{SRFA}])$. [b] $R^2$ is the correlation coefficient.

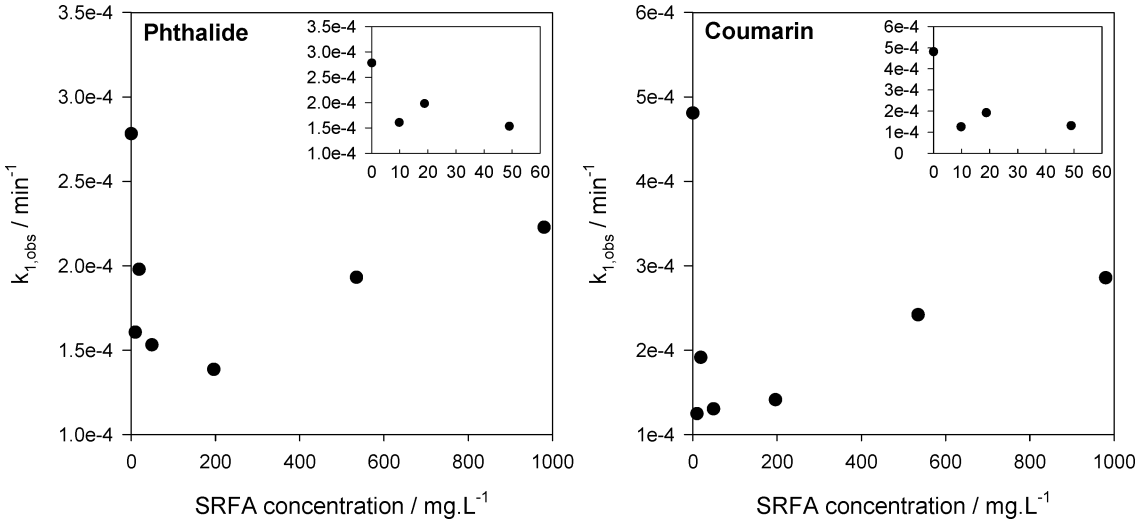


**Figure 6.** Effect of SRFA on the observed formation rate constants for phthalide and coumarin in a 22 $\mu$m aqueous film. The insets are blowups of the data at small SRFA concentrations.

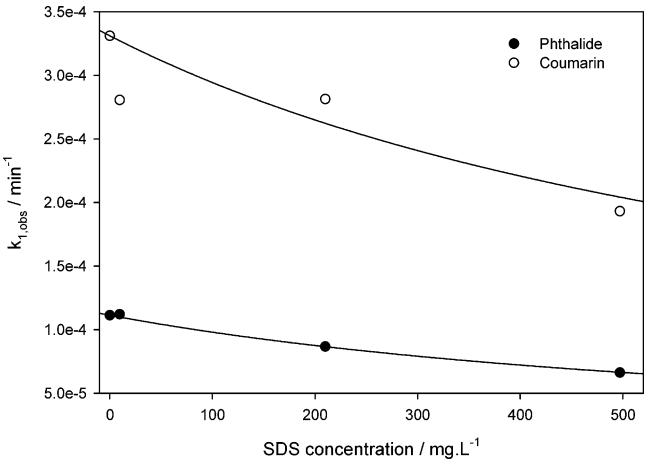


**Figure 7.** Effect of SDS on the observed formation rate constants for phthalide and coumarin in a 450 $\mu$m aqueous film. The solid lines represent the theoretical fit to experimental data (eq 9).

the 450 $\mu$m SDS aqueous solution film was also investigated. Figure 7 shows the observed formation rate constants for phthalide and coumarin in the 450 $\mu$m film as a function of the SDS concentration. Unlike SRFA, SDS was photochemically inert under the UV light we used and did not show a significant effect on the photooxidation of naphthalene as SRFA did. Only at SDS concentrations as high as 500 mg·L$^{-1}$ was an obvious decrease in the formation rate constants observed. The reason for the suppression of naphthalene photooxidation at high SDS concentrations could be that a considerable portion of naphthalene molecules are bound to SDS molecules at high SDS concentrations and become insusceptible to singlet oxygen attack. The following expression of the formation rate constant is obtained on the basis of this assumption (see Supporting Information for derivation):

$$k_{1,obs} = k^0_{1,obs} \frac{1}{1 + K_{OM}[SDS]} \quad (9)$$

Here $k^0_{1,obs}$ is the formation rate constant in pure water. By fitting the kinetic data to this equation, we obtain an average $K_{OM}$ value of $1.31 \times 10^{-3}$ L·mg$^{-1}$ for SDS, equal to $2.62 \times 10^{-3}$ L·(mg of carbon)$^{-1}$, which is in good agreement with the average $K_{OM}$ value obtained from SRFA ($2.77 \times 10^{-3}$ L·(mg of carbon)$^{-1}$). Because of their chemical similarity, the effect of SDS on the photooxidation of naphthalene is suggestive of that of naturally occurring long chain fatty acids.[11]

**Atmospheric Implications.** Fog samples collected in the Po Valley of Italy, an area reported to have high levels of pollution, revealed high concentrations of water-soluble organic compounds (WSOC) in fog droplets, ranging between 14 and 108 mg of carbon·L$^{-1}$.[43−45] The humic-like polyacidic compounds were found to represent an average 25% of the WSOC, and their concentrations were estimated to range between 3.5 and 27 mg of carbon·L$^{-1}$, corresponding to concentrations of 6.7−51.5 mg·L$^{-1}$ for the surrogate SRFA. As shown in our work, SRFA suppresses the photooxidation of naphthalene over this atmospherically relevant concentration range even though the surface reaction enhancement is greater in the presence of SRFA over this range than in pure water. In addition to photochemical reactions, PAHs in thin atmospheric water films are subject to various other oxidation processes initiated by reactive oxygen species in the atmosphere, including, for instance, •OH, •$NO_3$, and $O_3$. Previous work from our laboratory showed that, contrary to the inhibiting effect of SRFA on the $^1O_2$ photooxidation of naphthalene over the atmospherically relevant SRFA concentration range, the presence of SRFA on the surface of micrometer-size water droplets was conducive to the trapping of $O_3$ and naphthalene and increased the ozonation rate of naphthalene by approximately 1 order of magnitude.[18] Although it is difficult to generalize the effect of SRFA on the oxidation of PAHs via different processes, it is doubtless that the presence of SRFA or HULIS in thin atmospheric water films significantly affects the fate of PAHs in the atmosphere.

**Acknowledgment.** This work was supported by a grant from the National Science Foundation (ATM 0355291). We also thank Prof. James Henry for allowing us to use the spectrofluorometer.

**Supporting Information Available:** Derivation of the product formation rates. This material is available free of charge via the Internet at http://pubs.acs.org.

## References and Notes

(1) Dobson, C. M.; Ellison, G. B.; Tuck, A. F.; Vaida, V. *Proc. Nat. Acad. Sci. U.S.A.* **2000**, *97*, 11864.

(2) Gill, P. S.; Graedel, T. E.; Weschler, C. *J. Rev. Geophys. Space Phys.* **1983**, *21*, 903.

(3) Seidl, W. *Atmos. Environ.* **2000**, *34*, 4917.

(4) Latif, M. T.; Brimblecombe, P. *Environ. Sci. Technol.* **2004**, *38*, 6501.

(5) Cappiello, A.; De Simoni, E.; Fiorucci, C.; Mangani, F.; Palma, P.; Trufelli, H.; Decesari, S.; Facchini, M. C.; Fuzzi, S. *Environ. Sci. Technol.* **2003**, *37*, 1229.

(6) Capel, P. D.; Gunde, R.; Zurcher, F.; Giger, W. *Environ. Sci. Technol.* **1990**, *24*, 722.

(7) Donaldson, D. J.; Vaida, V. *Chem. Rev.* **2006**, *106*, 1445.

(8) Davies, J. T.; Rideal, E. K. *Interfacial Phenomena*, 2nd ed.; Academic Press, Inc.: New York, 1961.

(9) Thornton, J. A.; Abbatt, J. P. D. *J. Phys. Chem. A* **2005**, *109*, 10004.

(10) Mmereki, B. T.; Donaldson, D. J.; Gilman, J. B.; Eliason, T. L.; Vaida, V. *Atmos. Environ.* **2004**, *38*, 6091.

(11) McNeill, V. F.; Patterson, J.; Wolfe, G. M.; Thornton, J. A. *Atmos. Chem. Phys.* **2006**, *6*, 1635.

(12) Eliason, T. L.; Gilman, J. B.; Vaida, V. *Atmos. Environ.* **2003**, *38*, 1367.

(13) Sumner, A. L.; Menke, E. J.; Dubowski, Y.; Newberg, J. T.; Penner, R. M.; Hemminger, J. C.; Wingen, L. M.; Brauers, T.; Finlayson-Pitts, B. *J. Phys. Chem. Chem. Phys.* **2004**, *6*, 604.

(14) Vacha, R.; Jungwirth, P.; Chen, J.; Valsaraj, K. T. *Phys. Chem. Chem. Phys.* **2006**, *8*, 4461.

(15) Donaldson, D. J.; Mmereki, B. T.; Chaudhuri, S. R.; Handley, S.; Oh, M. *Faraday Discuss.* **2005**, *130*, 1.

(16) Mmereki, B. T.; Donaldson, D. J. *J. Phys. Chem. A* **2003**, *107*, 11038.

(17) Raja, S.; Valsaraj, K. T. *Environ. Sci. Technol.* **2004**, *38*, 763.

(18) Raja, S.; Valsaraj, K. T. J. *Air Waste Manage. Assoc.* **2005**, *55*, 1345.

(19) Raja, S.; Yaccone, F. S.; Ravikrishna, R.; Valsaraj, K. T. *J. Chem. Eng. Data* **2002**, *47*, 1213.

(20) Raja, S.; Valsaraj, K. T. J. *Air Waste Manage. Assoc.* **2004**, *54*, 1550.

(21) Chen, J.; Ehrenhauser, F. S.; Valsaraj, K. T.; Wornat, M. J. J. *Phys. Chem. A* **2006**, *110*, 9161.

(22) Gilman, J. B.; Vaida, V. J. *Phys. Chem. A* **2006**, *110*, 7581.

(23) Fasnacht, M. P.; Blough, N. V. *Environ. Sci. Technol.* **2002**, *36*, 4364.

(24) Bertilsson, S.; Widenfalk, A. *Hydrobiologia* **2002**, *469*, 23.

(25) Montgomery, J. H. *Groundwater Chemicals: Desk Reference*, 2nd ed.; CRC Press/Lewis Publishers: Boca Raton, FL, 1996.

(26) Sander, R. *Henry's Law data*, 69th ed.; U.S. Department of Commerce: Gaithersburg, MD, 2005.

(27) Alaee, M.; Whittal, R. M.; Strachan, W. M. J. *Chemosphere* **1996**, *32*, 1153.

(28) Rana, D.; Neale, G. H.; and Hornof, V. *Colloid Polym. Sci.* **2002**, *280*, 775.

(29) Browne, B. A.; and Driscoll, C. T. *Environ. Sci. Technol.* **1993**, *27*, 915.

(30) Thorn, K. A.; Folan, D. W.; and MacCarthy P. Characterization of the International Humic Substances Society Standard and Reference Fulvic and Humic Acids by Solution State Carbon-13 (13C) and Hydrogen-1 (1H) Nuclear Magnetic Resonance Spectrometry, U.S. Geological Survey, Water-Resources Investigations Rep. 89-4196, 1989.

(31) Hayase, K.; Tsubota, H. *Geochim. Cosmochim. Acta* **1983**, *47*, 947.

(32) Valsaraj, K. T. *Elements of Environmental Engineering: Thermodynamics and Kinetics*, 2nd ed.; CRC Press/Lewis Publishers: Boca Raton, FL, 2000.

(33) Zepp, R. G.; Schlotzhauer, P. F.; Sink, R. M. *Environ. Sci. Technol.* **1985**, *19*, 74.

(34) Vione, D.; Maurino, V.; Minero, C.; Pelizzetti, E.; Harrison.; M. A. J.; Olariu.; R. I.; Arsene, C. *Chem. Soc. Rev.* **2006**, *35*, 441.

(35) Suzdorf, A. R.; Morozov, S. V.; Kuzubova, L. I.; Anshits, N. N.; Anshits, A. G. *Chem. Sustainable Dev., Part 2* **1994**, *2-3*, 449.

(36) Haag, W. R.; Hoigne, J. *Environ. Sci. Technol.* **1986**, *20*, 341.

(37) Latch, D. E.; McNeill, K. *Science* **2006**, *311*, 1743.

(38) Schlautman, M. A.; Morgan, J. J. *Environ. Sci. Technol.* **1993**, *27*, 961.

(39) Canonica, S.; Hoigne, J. *Chemosphere* **1995**, *30*, 2365.

(40) Murov, S. L.; Carmichael, I.; Hug, G. L. *Handbook of photochemistry*, 2nd ed.; Marcel Dekker: New York, 1993.

(41) Nissenson, P.; Knox, C. J. H.; Finlayson-Pitts, B. J.; Phillips, L. F.; Dabdub, D. *Phys. Chem. Chem. Phys.* **2006**, *8*, 4700.

(42) Remorov., R. G.; George, C. *Phys. Chem. Chem. Phys.* **2006**, *8*, 4897.

(43) Facchini, M. C.; Mircea, M.; Fuzzi, S.; Charlson, R. J. *Nature* **1999**, *401*, 257.

(44) Gelencser, A.; Sallai, M.; Krivacsy, Z.; Kiss, G.; Meszaros, E. *Atmos. Res.* **2000**, *54*, 157.

(45) Facchini, M. C.; Decesari, S.; Mircea, M.; Fuzzi, S.; Loglio, G. *Atmos. Environ.* **2000**, *34*, 4853.